Control of population transfer in a multilevel Li$_2$ molecule by stimulated hyper-Raman nonadiabatic passage with chirped laser pulses

Chitrakshya Sarkar, Rangana Bhattacharya, S. S. Bhattacharyya, and Samir Saha

Atomic and Molecular Physics Section, Department of Materials Science, Indian Association for the Cultivation of Science,
Jadavpur, Kolkata 700032, India
(Received 17 April 2008; published 14 August 2008)

We have theoretically studied the population transfer in a five-level Li$_2$ dimer by (2+2)-photon stimulated hyper-Raman nonadiabatic passage (STIHRNAP) from the initial ground level $v_g=0$, $J_g=0$ to the final rovibrational levels $v_f=1$ (2), $J_f=0,2$, of the ground electronic state $X\,{}^1\Sigma_g^+$ via the resonant intermediate levels $v_i=1$, $J_i=0,2$, of the excited electronic state $2\,{}^1\Sigma_g^+$. Linearly chirped pump and Stokes laser pulses with different chirp rates and without any initial detuning are applied simultaneously. Both the pulses are taken to have the same temporal shape, pulse width, and linear parallel polarizations. The density matrix method has been used to compute the populations of the levels. We have investigated in detail the population transfer for laser wavelengths (at time $t=0$) in the range of 992–1028 nm and (peak) intensities in the range of 1.5×10^{10}–3.0×10^{11} W/cm^2. The required pulse widths are of the order of 35–275 ps for maximum population inversion. We have controlled rotational branching in population transfer to the final rotational levels $J_f=0$ (Q branch) and $J_f=2$ (S branch) of the fundamental ($v_f=1$) and first overtone ($v_f=2$) transitions by judicious choice of laser parameters. We have applied a (2+2)-photon STIHRNAP process to a model multilevel molecular system (Li$_2$) and achieved almost complete population transfer from the initial ground to the final target rovibrational levels with chirped ir laser pulses.

I. INTRODUCTION

In recent years, coherent control of efficient and selective transfer of population in atomic or molecular levels by interaction with well-tailored laser pulses has been an important area of study. Coherent population transfer by the process of stimulated Raman adiabatic passage (STIRAP) [1–4] is one such control scheme that has been extensively investigated over the past decade and fairly well understood by now. In STIRAP, partially overlapping pump and Stokes laser pulses in counterintuitive sequence couple the initial and final state levels via the intermediate resonant state level by two single-photon transitions. For small diatomic Raman active molecules, like H$_2$, N$_2$, O$_2$, the pump and Stokes field couplings to the (allowed) first excited (resonant intermediate) electronic state require high-energy [extreme ultraviolet (xuv) or vacuum ultraviolet (vuv)] photons. Laser pulses in this spectral zone with adequate power and pulse widths required for adiabatic passage may be experimentally difficult to tailor or design. This difficulty can be avoided when the (1+1)-photon Raman process (one-photon couplings at two steps) in STIRAP is replaced by a (2+2)-photon Raman process (two-photon couplings at two steps). This extension from Raman to hyper-Raman process at one or two steps is called stimulated hyper-Raman adiabatic passage (STIHRAP) which was first proposed in a pioneering work by Yatsenko *et al.* [5] for efficient population transfer to excited states of atoms [5–7]. However, in STIHRAP, the dynamic Stark shifts of the state levels connected in the two-photon transitions are to be considered, since the ac Stark shifts, like the driving two-photon Rabi frequencies, are proportional to the intensities of the laser fields. Therefore, in STIHRAP, the dynamic Stark shifts cannot be eliminated and it is difficult to obtain values of control parameters of laser pulses for efficient population transfer.

Another control scheme is the Raman chirped adiabatic passage (RCAP) which uses chirped laser pulses [8–10]. In RCAP, both the pump and Stokes laser frequencies are far from one-photon resonance but are swept through two-photon resonance for transition from the initial to the final target levels. Davis and Warren [9] have used the density matrix technique to include rotational effects in the high vibrational excitation of O$_2$ and Cl$_2$ by RCAP. Thomas *et al.* [11] have investigated rovibrational state selectivity by chirped adiabatic passage of dynamically laser-aligned molecules and achieved complete excitation of the chosen state of CO by infrared or Raman process. Légaré *et al.* [12] have studied the Raman chirped nonadiabatic passage (RCNAP) by (1+1)-photon Raman transitions in H$_2$. Here, population transfer from the ground rovibrational level to higher rovibrational levels of the ground electronic $X\,{}^1\Sigma_g^+$ state via the resonant intermediate $B\,{}^1\Sigma_u^+$ excited electronic state of H$_2$ molecule was demonstrated by rapid linear chirpings of the simultaneously applied pump and Stokes laser pulses. This led to nonadiabatic passage between adiabatic (dressed) states of the Raman process. Optimum population inversion was achieved by controlling the interference between resonant nonadiabatic and nonresonant adiabatic pathways due to initial detunings of the chirped laser pulses.

Very recently, we have studied the population inversion to the excited final vibrational levels $v_f=1,2$, with $J_f=0$ from the initial ground level $v_g=0$, $J_g=0$ of the ground electronic $X\,{}^1\Sigma_g^+$ state of H$_2$ via resonant intermediate $EF\,{}^1\Sigma_g^+$ excited electronic state by (2+2)-photon stimulated hyper-Raman process with linearly chirped pump and Stokes laser pulses [13]. In the work, both the pump and Stokes fields without any initial detuning were applied simultaneously and population transfer took place by nonadiabatic transition between the initial and final adiabatic states.

In the present paper, we have investigated the population transfer in a model multilevel Li_2 alkali dimer from the initial ground level $v_g=0$, $J_g=0$ to the final excited rovibrational levels $v_f=1,2$, $J_f=0,2$ of the ground electronic state $X\ ^1\Sigma_g^+$. The transfer takes place via resonant intermediate rovibrational levels $v_i=1$, $J_i=0,2$, of the excited electronic state $2\ ^1\Sigma_g^+$ by (2+2)-photon stimulated hyper-Raman nonadiabatic passage (STIHRNAP). As before [13], linearly chirped pump and Stokes laser pulses were used. In this work, our motivation was to find out if and how efficient and selective population transfer to a desired final level in the multilevel Li_2 molecular system can be achieved by manipulation of suitable control parameters such as intensities, frequencies, pulse durations, and chirp rates of the laser pulses. However, in Li_2, it is essential to consider more levels than in H_2 [13] for this kind of process and this makes the search for the optimal parameters for the laser-induced population transfer process more difficult.

In Li_2, owing to its higher mass, the excited electronic state energies are much more closely spaced compared to H_2. Here, the rovibrational levels of the ground electronic $X\ ^1\Sigma_g^+$ state of Li_2 can resonantly couple to the rovibrational levels of the excited electronic state $2\ ^1\Sigma_g^+$ by two-photon ir transitions. Hence, the pump and Stokes laser parameters are experimentally more feasible due to their lower frequencies in comparison to those in the case of the H_2 molecule where photons (~ 200 nm wavelength) in the uv range were required to connect the ground level ($v_g=0$, $J_g=0$) of the ground electronic state $X\ ^1\Sigma_g^+$ to the rovibrational level ($v_i=6$, $J_i=0$) of the resonant intermediate electronic state $EF\ ^1\Sigma_g^+$ by two-photon couplings [13]. It is also worthwhile to mention here that in Li_2 with photon wavelength (~ 1000 nm) in the ir range, it would require five photons (energy ~ 1.24 eV) to reach the ionization threshold (5.145 eV) [14] of the Li_2 molecule and hence the population loss due to ionization can be made negligible for this alkali dimer using suitable laser parameters. The H_2 molecule is more susceptible to ionization than Li_2 due to more easily accessible ionization threshold (15.426 eV) [14] of H_2 by photons (energy ~ 6.20 eV) in the uv range. Keeping in view these advantages, the Li_2 alkali dimer has been chosen as a model multilevel molecular system for the present study of population transfer by the STIHRNAP process.

In Sec. II, we present the formulation of the five-level Li_2 system using the density matrix method. In Sec. III, we briefly discuss the ways the calculations have been performed and the various parameters used in the calculations. In Sec. IV, we illustrate and discuss the results. Finally, in Sec. V, we give a brief conclusion.

II. FORMULATION

The scheme of the population transfer process in the model five-level Li_2 alkali dimer by (2+2)-photon stimulated hyper-Raman process is shown in Fig. 1. The pump pulse connects the rovibrational level $v_g=0$, $J_g=0$ of the ground electronic state $X\ ^1\Sigma_g^+$ to the rovibrational levels $v_i=1$, $J_i=0,2$, of the intermediate resonant excited electronic state $2\ ^1\Sigma_g^+$ by a two-photon transition. The Stokes pulse
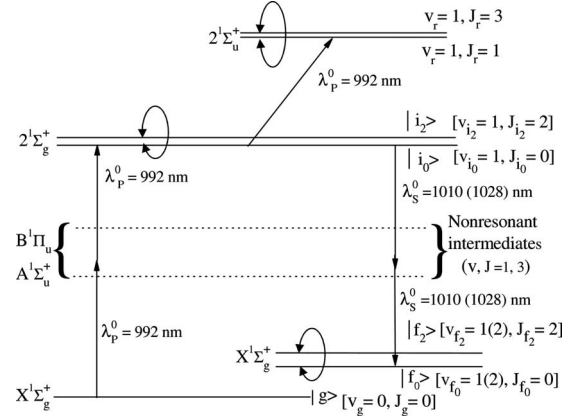

FIG. 1. Schematic energy-level diagram showing the relevant electronic states of Li_2 molecule for (2+2)-photon stimulated hyper-Raman process with initial ($t=0$) wavelengths λ_P^0 and λ_S^0 of the pump and Stokes laser pulses. The couplings between the two closely spaced (rotational) levels in different electronic states are also indicated.

similarly connects the levels $v_i=1$, $J_i=0,2$, of the $2\ ^1\Sigma_g^+$ state to the final higher rovibrational levels $v_f=1$ (2), $J_f=0,2$, of the $X\ ^1\Sigma_g^+$ state by another two-photon transition. The pump and Stokes pulses are applied simultaneously without any initial ($t=0$) detuning of the chirped pulses. We have utilized the density matrix technique for this five-level Li_2 molecular system interacting with the two applied laser fields.

The Liouville equation of motion of the density matrix is given by (in a.u.)

$$\frac{d\rho(t)}{dt} = -i[H(t),\rho(t)] - \Gamma\rho(t), \tag{1}$$

where $\rho(t)$ is the density matrix of the system with 25 elements. The diagonal elements ρ_{jj} give the populations of the five levels whereas the off-diagonal elements are the coherence terms. Here, $H(t)=H_0+H_I(t)$ is the total Hamiltonian of the system, where H_0 is the Hamiltonian of the unperturbed molecule plus the laser fields and $H_I(t)$ is the interaction Hamiltonian between the molecule and the fields. The last term in Eq. (1) accounts for the spontaneous or induced (photoionization or photodissociation) population decay from the resonant intermediate levels of the molecule. The interaction Hamiltonian $H_I(t)$ in the electric field gauge (with dipole approximation) is

$$H_I(t) = -\vec{E}_P(t)\cdot\vec{d} - \vec{E}_S(t)\cdot\vec{d}, \tag{2}$$

where $\vec{E}_P(t)$ and $\vec{E}_S(t)$ are electric fields of the pump and Stokes pulses, respectively. $\vec{d}$ is the electric transition dipole operator. We have considered linear parallel polarizations of the pump and Stokes laser fields. The fields are given by

$$\vec{E}_{P,S}(t) = \hat{\varepsilon}_{P,S}f_{P,S}(t)(I_{P,S}^0)^{1/2}\cos[\phi_{P,S}(t)]. \tag{3}$$

Here, $f_{P,S}(t)$ specify the envelopes of the pump and Stokes fields with peak amplitudes $(I_P^0)^{1/2}$ and $(I_S^0)^{1/2}$. $\hat{\varepsilon}_{P,S}$ give the

directions of polarizations of the fields. $\phi_{P,S}(t)$ are the phases of the fields. The instantaneous frequencies $\omega_{P,S}(t)$ of the chirped laser fields are the time derivatives of the phase $\phi_{P,S}(t)$ [8,11,15],

$$\omega_{P,S}(t) = \frac{d\phi_{P,S}(t)}{dt}. \qquad (4)$$

The amplitude envelopes of the fields are taken as

$$f_{P,S}(t) = \sin^2[\pi t/(2\tau_{P,S})], \qquad (5)$$

where τ_P and τ_S are the full widths at half-maximum (FWHM) of the pump and Stokes pulses, respectively.

The ac Stark shift of the initial ground (g) level due to the pump (P) pulse is

$$S_g^P(t) = \sum_{vJ} |\Omega_{vJ,g}^P(t)|^2/(E_g + \omega_P - E_{vJ})$$
$$+ \sum_{vJ} |\Omega_{vJ,g}^P(t)|^2/(E_g - \omega_P - E_{vJ}). \qquad (6)$$

The shift $S_g^S(t)$ due to the Stokes (S) pulse can be expressed similarly. We denote $S_g(t) = S_g^P(t) + S_g^S(t)$. Similar expressions of the ac Stark shifts $S_{i_0}(t)$ and $S_{i_2}(t)$ for the resonant intermediate (i) rovibrational levels $(v_i=1, J_i=0$ and $2)$ of the excited electronic state $2\,^1\Sigma_g^+$, and $S_{f_0}(t)$ and $S_{f_2}(t)$ for the final (f) rovibrational levels $[v_f=1\,(2), J_f=0$ and $2]$ of the electronic state $X\,^1\Sigma_g^+$ (Fig. 1) were taken into account. To calculate the Stark shifts $S_{i_2}(t)$ for $J_i=2$ and $S_{f_2}(t)$ for $J_f=2$, the contributions of both of the nonresonant rotational levels $J=1$ and 3 were considered in accordance with the rotational selection rule. The first term in Eq. (6) is the RWA (rotating wave approximation) and the second term is the counter-RWA contributions. $\Omega_{vJ,g}^P(t)$ are the one-photon Rabi frequencies between the ground vibrational-rotational level (g) and the various vibrational-rotational levels (vJ) of the nonresonant intermediate $A\,^1\Sigma_u^+$, $B\,^1\Pi_u$, $2\,^1\Sigma_u^+$ electronic states coupled by the pump pulse satisfying the rotational selection rule. During the calculation of the one-photon matrix elements Ω, the numerically generated vibrational wave functions of various electronic states and the spherical harmonic rotational states have been used as the basis states. The variation of the electronic transition dipole moments with internuclear separation was taken into account.

The two-photon Rabi frequency between the initial level $v_g=0$, $J_g=0$ of the ground electronic state $X\,^1\Sigma_g^+$ to the resonant intermediate $2\,^1\Sigma_g^+$ state level i_0 $(v_i=1, J_i=0)$ due to the pump (P) photon (Fig. 1) is (in RWA)

$$\tilde{\Omega}_{i_0g}^P(t) = \sum_{vJ} \Omega_{i_0,vJ}^P(t)\Omega_{vJ,g}^P(t)/(E_g + \omega_P - E_{vJ}). \qquad (7)$$

Similar is the expression of $\tilde{\Omega}_{i_2g}^P(t)$ for the resonant intermediate $2\,^1\Sigma_g^+$ state level i_2 $(v_i=1, J_i=2)$. Similarly, we can express $\tilde{\Omega}_{i_0f_0}^S(t)$ and $\tilde{\Omega}_{i_2f_2}^S(t)$ due to Stokes (S) pulse where $\tilde{\Omega}_{i_0f_0}^S(t)$ couples the resonant intermediate $2\,^1\Sigma_g^+$ state level i_0 $(v_i=1, J_i=0)$ to the final (f_0) level $v_f=1$ (2), $J_f=0$ of the ground electronic state $X\,^1\Sigma_g^+$ and $\tilde{\Omega}_{i_2f_2}^S(t)$ couples the resonant intermediate $2\,^1\Sigma_g^+$ state level i_2 $(v_i=1, J_i=2)$ to the final
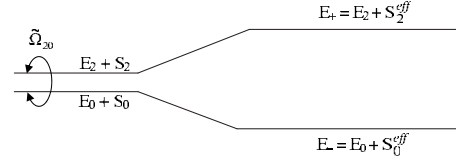

FIG. 2. Schematic energy-level diagram showing the dressing of two levels due to the coupling $(\tilde{\Omega}_{20})$ between the two levels.

(f_2) level $v_f=1$ (2), $J_f=2$ of the $X\,^1\Sigma_g^+$ state (Fig. 1). The two-photon Rabi frequencies $\tilde{\Omega}_{i_0f_2}^S(t)$ and $\tilde{\Omega}_{i_2f_0}^S(t)$ can be expressed in a similar way. All two-photon matrix elements have been calculated by summation over basis states which include all possible discrete vibrational-rotational level states of the relevant electronic states which can act as virtual intermediates. The counter-RWA terms in the two-photon Rabi frequency expressions were not considered as they are highly oscillatory and would not make any significant contribution.

We have also taken into account the relatively stronger two-photon couplings $\tilde{\Omega}_{i_2i_0}(t)$ and $\tilde{\Omega}_{f_2f_0}(t)$ between the very closely spaced (few cm^{-1}) rotational levels $J_i=0$ and $J_i=2$ of the vibrational level $v_i=1$ of the resonant intermediate electronic state $2\,^1\Sigma_g^+$, and between $J_f=0$ and $J_f=2$ of the final excited vibrational levels $v_f=1$ (2) of the ground electronic state $X\,^1\Sigma_g^+$ (Fig. 1). The two-photon coupling between the closely spaced rotational levels $J=0$ and $J=2$ of the electronic state $2\,^1\Sigma_g^+$ or $X\,^1\Sigma_g^+$ due to pump (P) pulse is

$$\tilde{\Omega}_{20}^P(t) = \sum_{vJ} \Omega_{2,vJ}^{P*}(t)\Omega_{vJ,0}^P(t)/(E_0 + \omega_P - E_{vJ})$$
$$+ \sum_{vJ} \Omega_{2,vJ}^P(t)\Omega_{vJ,0}^{P*}(t)/(E_0 - \omega_P - E_{vJ}). \qquad (8)$$

Similar would be the expression of $\tilde{\Omega}_{20}^S(t)$ due to the Stokes (S) pulse. We write $\tilde{\Omega}_{20}(t) = \tilde{\Omega}_{20}^P(t) + \tilde{\Omega}_{20}^S(t)$. The first term in Eq. (8) is the RWA while the second term is the counter-RWA contributions. The single-photon matrix elements have been calculated in the same way as mentioned earlier. It may be noticed that Eq. (8) is unlike the two-photon Rabi frequency [viz., Eq. (7)] between rovibrational levels of two different electronic states but is like the dynamic Stark shift [viz., Eq. (6)] of a rovibrational level in an electronic state. These two-photon strong couplings under the presence of pump and Stokes laser fields play an important role by dressing the very closely spaced energy levels. Thus, for the hyper-Raman process in a multilevel system (Fig. 1), in contrast to the hyper-Raman process in a three-level system treated earlier [13], we have two different terms that account for the dressing of the rovibronic levels (i_0, i_2) and (f_0, f_2); one due to the usual two-photon Stark shifts of the levels and the other due to the two-photon couplings between the closely spaced levels. With the inclusion of dynamic Stark shifts, two-photon couplings between the closely spaced rotational levels and two-photon RWA Rabi frequencies, the form of the Hamiltonian of the five-level system (Fig. 1) may be written as

$$H(t) = \begin{pmatrix} E_g + S_g(t) + 2\omega_P(t) & \widetilde{\Omega}^P_{i_0 g}(t) & \widetilde{\Omega}^P_{i_2 g}(t) & 0 & 0 \\ \widetilde{\Omega}^P_{i_0 g}(t) & E_{i_0} + S_{i_0}(t) - i\Gamma_{i_0} & \widetilde{\Omega}^{P+S}_{i_0 i_2}(t) & \widetilde{\Omega}^S_{i_0 f_0}(t) & \widetilde{\Omega}^S_{i_0 f_2}(t) \\ \widetilde{\Omega}^P_{i_2 g}(t) & \widetilde{\Omega}^{P+S}_{i_0 i_2}(t) & E_{i_2} + S_{i_2}(t) - i\Gamma_{i_2} & \widetilde{\Omega}^S_{f_0 i_2}(t) & \widetilde{\Omega}^S_{f_2 i_2}(t) \\ 0 & \widetilde{\Omega}^S_{i_0 f_0}(t) & \widetilde{\Omega}^S_{f_0 i_2}(t) & E_{f_0} + S_{f_0}(t) + 2\omega_S(t) & \widetilde{\Omega}^{P+S}_{f_0 f_2}(t) \\ 0 & \widetilde{\Omega}^S_{i_0 f_2}(t) & \widetilde{\Omega}^S_{f_2 i_2}(t) & \widetilde{\Omega}^{P+S}_{f_0 f_2}(t) & E_{f_2} + S_{f_2}(t) + 2\omega_S(t) \end{pmatrix}. \tag{9}$$

The effective Stark shifts of the two closely spaced rotational levels (dressed) can be determined from the mathematical expressions [16] of the dressed energy levels (Fig. 2), taking into account the normal or usual Stark shifts of the levels, given by

$$E_\pm = [(E_2 + S_2) + (E_0 + S_0)]/2 \pm \{[(E_2 + S_2) - (E_0 + S_0)]^2 + 4|\widetilde{\Omega}_{20}|^2\}^{1/2}/2, \tag{10}$$

where E_2, E_0 ($E_2 > E_0$) are the unperturbed eigenenergies of the two levels, S_2 and S_0 are the usual two-photons Stark shifts of the energy levels E_2 and E_0, respectively. $\widetilde{\Omega}_{20} = \widetilde{\Omega}_{i_2 i_0}$ or $\widetilde{\Omega} f_0 f_2$ is the two-photon coupling between the two closely spaced rotational levels (E_2 and E_0) of the same vibronic state. Thus, the effective Stark shifts of the closely spaced two levels are

$$S_2^{\text{eff}} = E_+ - E_2 \tag{11a}$$

and

$$S_0^{\text{eff}} = E_- - E_0. \tag{11b}$$

We consider linear chirpings of the pulses so that the frequencies vary as

$$\omega_P(t) = \omega_P^0 + c_r^P t \tag{12a}$$

and

$$\omega_S(t) = \omega_S^0 + c_r^S t, \tag{12b}$$

where ω_P^0 and ω_S^0 are initial ($t=0$) frequencies while c_r^P and c_r^S are the chirp rates of the pump and Stokes lasers, respectively. From Eqs. (11) and following our earlier paper [13], we have judiciously determined the possible chirp rates of the pulses for efficient population transfer. We take the chirp rates in the forms

$$c_r^P = \beta_P[(S_{i_{2,0}}^{\text{eff}})^0 - S_g^0]/\tau_P \tag{13a}$$

and

$$c_r^S = \beta_S[(S_{i_{2,0}}^{\text{eff}})^0 - (S_{f_{2,0}}^{\text{eff}})^0]/\tau_S, \tag{13b}$$

where β_P and β_S are the dimensionless chirp rate parameters ($0 < \beta_{P,S} < 1$). $(S_{i_{2,0}}^{\text{eff}})^0$ and $(S_{f_{2,0}}^{\text{eff}})^0$ are the effective Stark shifts of the resonant intermediate state levels i_2 or i_0 and final state levels f_2 or f_0, respectively, at the values of the peak intensities ($I_{P,S}^0$). S_g^0 is the normal Stark shift of the ground-state

level (g) at $I_{P,S}^0$. We have optimized the values of β_P, β_S for given peak values ($I_{P,S}^0$) of intensities and pulse widths ($\tau_{P,S}$) of the pulses to maximize the population transfer to the final levels $v_f = 1, 2$ with $J_f = 1, 2$.

From the Liouville equation (1), the optical Bloch equations for the slowly varying density matrix operator $\sigma(t)$ [17] are obtained by using the RWA [4,10]. We adiabatically eliminate [18] the density matrix elements involving the nonresonant rovibrational levels of the intermediate electronic states. Then, we obtain a set of 25 equations which can be expressed in a compact form as

$$\frac{d\sigma(t)}{dt} = M(t)\sigma(t) - \Gamma\sigma(t), \tag{14}$$

where $M(t)$ is a non-Hermitian but symmetric matrix [19] of 25×25 dimension. The diagonal elements of $M(t)$ contain the normal dynamic Stark shifts of the levels concerned which are proportional to the intensities. The off-diagonal matrix elements of $M(t)$ contain the two-photon Rabi frequencies and the two-photon couplings (between the closely spaced rotational levels) which are also proportional to the intensities.

It may be pointed out here that we have solved the density matrix equations of the five-level molecular system by directly incorporating the two-photon coupling terms (between the closely spaced levels) in the 25×25 $M(t)$ matrix. Separate diagonalization of the 2×2 matrix representing the closely spaced rotational levels along with their two-photon couplings was necessary only to get an estimate of the required chirp rates [Eq. (13)] through their effective Stark shifts at the peak laser intensities. During this estimation, we have neglected the interaction with the other remaining (three) levels (Fig. 1). We could do so without appreciable error since the two-photon Rabi frequencies between the levels of the different electronic states are much smaller than the two-photon couplings between the two closely spaced levels in the same electronic state (Table I).

III. CALCULATIONS

We have calculated the population transfer from the initial ground level $v_g = 0$, $J_g = 0$ to the final target levels $v_f = 1$ (2), $J_f = 0, 2$, of the ground electronic state $X\,^1\Sigma_g^+$ via resonant intermediate levels $v_i = 1$, $J_i = 0, 2$, of the excited electronic state $2\,^1\Sigma_g^+$ of the model five-level Li_2 molecular system (Fig.

TABLE I. Values (in cm^{-1}) of the two-photon Rabi frequencies, two-photon couplings, and dynamic Stark shifts for pump and Stokes pulses corresponding to the final levels $v_f=1$, $J_f=0,2$ and $v_f=2$, $J_f=0,2$ of Li$_2$ molecule. $\Gamma_{i_{0,2}}$ are the spontaneous decay widths (in cm^{-1}) of the resonant intermediate levels and $I_{P,S}$ are the pump and Stokes pulse intensities in W/cm^2.

	$v_f=1$, $J_f=0,2$	$v_f=2$, $J_f=0,2$
$\tilde{\Omega}_{i_0 g}^{P}$	$-5.18[-12]I_P$[a]	$-5.18[-12]I_P$
$\tilde{\Omega}_{i_2 g}^{P}$	$-4.03[-12]I_P$	$-4.03[-12]I_P$
$\tilde{\Omega}_{i_0 f_0}^{S}$	$-1.56[-11]I_S$	$-3.25[-11]I_S$
$\tilde{\Omega}_{i_0 f_2}^{S}$	$-1.22[-11]I_S$	$-2.57[-11]I_S$
$\tilde{\Omega}_{i_2 f_0}^{S}$	$-1.22[-11]I_S$	$-2.57[-11]I_S$
$\tilde{\Omega}_{i_2 f_2}^{S}$	$-2.34[-11]I_S$	$-4.89[-11]I_S$
$\tilde{\Omega}_{i_0 i_2}$	$-1.51[-9]I_P+2.91[-9]I_S$	$-1.51[-9]I_P-1.04[-9]I_S$
$\tilde{\Omega}_{f_0 f_2}$	$-1.78[-10]I_P-1.70[-10]I_S$	$-1.96[-10]I_P-1.78[-10]I_S$
S_g	$-5.06[-10]I_P-4.95[-10]I_S$	$-5.06[-10]I_P-4.85[-10]I_S$
S_{i_0}	$-1.69[-9]I_P+3.25[-9]I_S$	$-1.69[-9]I_P-1.16[-9]I_S$
S_{i_2}	$-2.66[-9]I_P+5.12[-9]I_S$	$-2.66[-9]I_P-1.83[-9]I_S$
S_{f_0}	$-5.29[-10]I_P-5.16[-10]I_S$	$-5.53[-10]I_P-5.27[-10]I_S$
S_{f_2}	$-6.42[-10]I_P-6.25[-10]I_S$	$-6.78[-10]I_P-6.40[-10]I_S$
$\Omega_{j_1 i_0}^{P}$	$-1.30[-10](I_P)^{1/2}$	$-1.30[-10](I_P)^{1/2}$
$\Omega_{j_j i_2}^{P}$	$-1.16[-10](I_P)^{1/2}$	$-1.16[-10](I_P)^{1/2}$
$\Omega_{j_3 i_2}^{P}$	$-1.14[-10](I_P)^{1/2}$	$-1.14[-10](I_P)^{1/2}$
Γ_{i_0}	$3.17[-5]$	$3.17[-5]$
Γ_{i_2}	$3.17[-5]$	$3.17[-5]$

[a]$-5.18[-12]=-5.18\times10^{-12}$.

1). The wavelength (λ_P^0) of the pump pulse at time $t=0$ is 992 nm while the wavelength (λ_S^0) of the Stokes pulse at $t=0$ for the final level $v_f=1$ (2) is 1010 (1028) nm. The peak intensities (I_P^0,I_S^0) of the pump and Stokes laser pulses with linear parallel polarizations are 3×10^{11} W/cm^2 and 1×10^{11} W/cm^2, respectively, for $v_f=1$, $J_f=0,2$, while I_P^0 and I_S^0 are 1×10^{11} W/cm^2 and 1.5×10^{10} W/cm^2, respectively,

for $v_f=2$, $J_f=0,2$. For maximum population transfer, the required pulse widths (τ_P,τ_S) for both the pulses are 35 ps for $v_f=1$, $J_f=0$ and 220 ps for $v_f=1$, $J_f=2$ while τ_P,τ_S are 275 ps for $v_f=2$, $J_f=0$ and 250 ps for $v_f=2$, $J_f=2$. The optimal values of the chirp rate parameters (β_P,β_S) with linear chirpings are very close to the "global" value of 0.53 (obtained for a three-level system [13]) for maximum population inversion.

The Born-Oppenheimer potential energies for the X $^1\Sigma_g^+$, A $^1\Sigma_u^+$, B $^1\Pi_u$, 2 $^1\Sigma_g^+$, and 2 $^1\Sigma_u^+$ electronic states of the Li$_2$ molecule are obtained from the comprehensive work of Schmidt-Mink *et al.* [20] who also give the transition electric dipole moments. The spontaneous relaxation rates of the resonant intermediate levels $v_i=1$, $J_i=0,2$, of the 2 $^1\Sigma_g^+$ electronic state are also taken from the same work. The potentials and the transition dipole moments are interpolated using the cubic spline interpolation method [21].

IV. RESULTS AND DISCUSSIONS

The two-photon Rabi frequencies, the two-photon couplings, the dynamic Stark shifts and the spontaneous decay widths of the levels concerned of the Li$_2$ molecular system are given in Table I. It is seen that the most important feature characterizing this system is that the magnitudes of the two-photon couplings between closely spaced rotational levels ($J=0,2$) and the ac Stark shifts are much larger than the two-photon Rabi frequencies. The populations of the initial ground (g), resonant intermediate (i), and the final (f) target levels at the end of the pulses for the peak intensities (I_P^0,I_S^0) and required pulse widths (τ_P,τ_S) of sin^2 pulses are shown in Table II for the final rovibrational levels $v_f=1,2$; $J_f=0,2$. The pump and Stokes photon wavelengths (λ_P^0,λ_S^0) at time $t=0$ are in the ir range and the chirp rate parameters (β_P,β_S) shown are the optimal values for maximum population inversion.

In Figs. 3 and 4, we have plotted against time (t) the relative effective ac Stark shifts of the resonant intermediate (i) levels $v_i=1$, $J_i=0,2$ with respect to the initial ground (g) and the final (f) target levels $v_f=1$, $J_f=0,2$ and $v_f=2$, J_f

TABLE II. Populations (P) of the initial ground ($v_g=0$, $J_g=0$), resonant intermediate ($v_i=0$, $J_i=0,2$), and final ($v_f=1,2$; $J_f=0,2$) rovibrational levels of Li$_2$ molecule at the end of the pulses for different peak intensities (I_P^0,I_S^0) and pulse widths (τ_P,τ_S) of the pump and Stokes laser fields. λ_P^0 and λ_S^0 are the laser wavelengths (at $t=0$). β_P and β_S are the dimensionless chirp rate parameters for the pump and Stokes lasers.

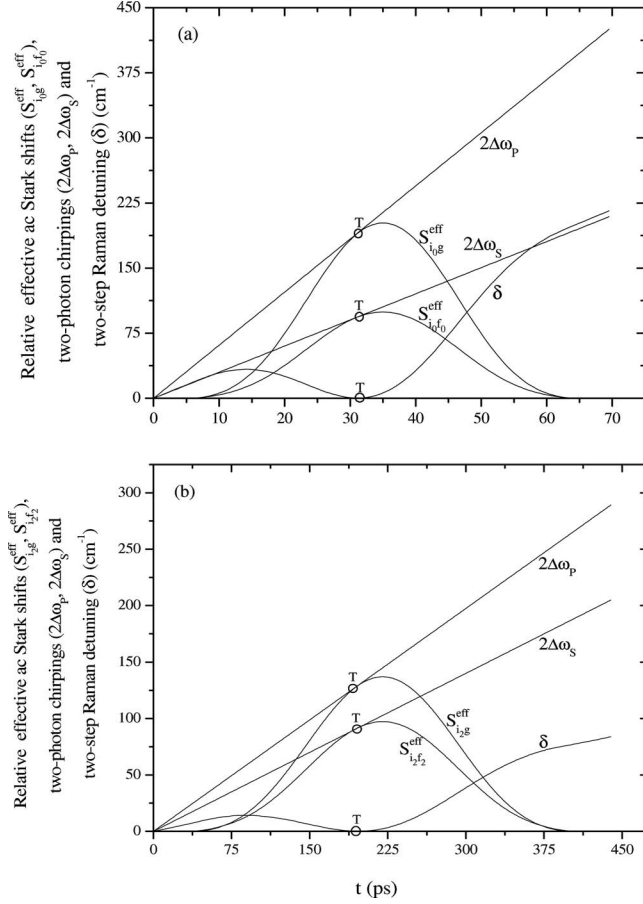|	$v_f=1$ $\lambda_P^0=992$ nm, $\lambda_S^0=1010$ nm $I_P^0=3.0\times10^{11}$ W/cm^2, $I_S^0=1.0\times10^{11}$ W/cm^2		$v_f=2$ $\lambda_P^0=992$ nm, $\lambda_S^0=1028$ nm $I_P^0=1.0\times10^{11}$ W/cm^2, $I_S^0=1.5\times10^{10}$ W/cm^2	
P (%)	$J_f=0$ $\tau_P=\tau_S=35$ ps $\beta_P=\beta_S=0.53$	$J_f=2$ $\tau_P=\tau_S=220$ ps $\beta_P=\beta_S=0.529$	$J_f=0$ $\tau_P=\tau_S=275$ ps $\beta_P=\beta_S=0.53$	$J_f=2$ $\tau_P=\tau_S=250$ ps $\beta_P=\beta_S=0.521$
P_g	1.2	4.0	0.0	3.3
P_{i_0}	0.6	0.0	0.2	0.0
P_{i_2}	0.2	1.3	0.0	9.2
P_{f_0}	95.3	0.0	99.8	0.0
P_{f_2}	2.7	94.7	0.0	87.5

FIG. 3. Relative effective ac Stark shifts, two-photon chirpings $(2\Delta\omega_P, 2\Delta\omega_S)$, and two-step Raman detuning (δ) with respect to ground $(v_g=0, J_g=0)$, resonant intermediate (v_i, J_i), and final (v_f, J_f) levels of Li$_2$ molecule as a function of time (t) with the optimal value of chirp rate parameters (β_P, β_S) for peak intensities $I_P^0=3.0\times10^{11}$ W/cm^2, $I_S^0=1.0\times10^{11}$ W/cm^2, and different pulse widths (τ_P, τ_S) of the pump and Stokes lasers. (a) $v_f=1, J_f=0; v_i=1, J_i=0, \tau_P=\tau_S=35$ ps and $\beta_P=\beta_S=0.53$. (b) $v_f=1, J_f=2; v_i=1, J_i=2, \tau_P=\tau_S=220$ ps and $\beta_P=\beta_S=0.529$.

$=0, 2$ respectively, caused by two different sets of peak intensities and different pulse widths. The relative effective ac Stark shift of the ground level $(v_g=0, J_g=0)$ with respect to the resonant intermediate level $(v_i=1, J_i=0)$ is

$$S_{i_0g}^{\text{eff}} = S_{i_0}^{\text{eff}} - S_g, \tag{15}$$

where the effective shifts of the concerned levels are given by Eqs. (11). Similar expressions of the relative effective ac Stark shifts $S_{i_2g}^{\text{eff}}, S_{i_0f_0}^{\text{eff}}, S_{i_2f_2}^{\text{eff}}$, etc., for the other relevant levels are obtained. As discussed earlier, the effective Stark shifts are derived by diagonalization of the 2×2 matrix which includes the strong two-photon couplings between the adjacent rotational levels. In the figures, we have also plotted the two-photon chirpings $(2\Delta\omega_P, 2\Delta\omega_S)$ of the pump and Stokes pulses, given by

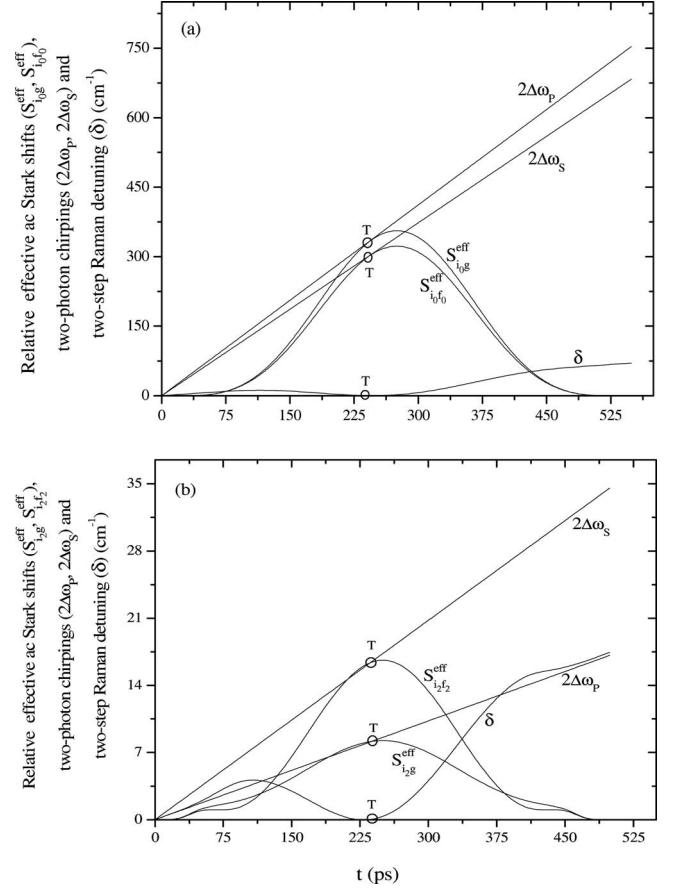$$2\Delta\omega_P = 2[\omega_P(t) - \omega_P^0] \tag{16a}$$

and

FIG. 4. Same as Fig. 3 except for $I_P^0=1.0\times10^{11}$ W/cm^2, $I_S^0=1.5\times10^{10}$ W/cm^2 and (a) $v_f=2, J_f=0; v_i=1, J_i=0, \tau_P=\tau_S=275$ ps and $\beta_P=\beta_S=0.53$. (b) $v_f=2, J_f=2; v_i=1, J_i=2, \tau_P=\tau_S=250$ ps and $\beta_P=\beta_S=0.521$.

$$2\Delta\omega_S = 2[\omega_S(t) - \omega_S^0], \tag{16b}$$

where $\omega_P(t), \omega_S(t)$ and ω_P^0, ω_S^0 are defined in Eq. (12). It is seen that the two-photon chirpings $(2\Delta\omega_P, 2\Delta\omega_S)$ touch the relative effective shift curves at a time T during the rising of the pulses with the optimal value of $\beta_P=\beta_S=0.53$ (0.529) for the final levels $v_f=1, J_f=0$ (2) and $\beta_P=\beta_S=0.53$ (0.521) for $v_f=2, J_f=0$ (2). At this time (T), Raman resonance occurs, i.e., the two-step $[(2+2)$-photon] Raman detuning $\delta(T)=0$, where

$$\delta(t) = [2\Delta\omega_P(t) - S_{i_0g}^{\text{eff}}(t)] - [2\Delta\omega_S - S_{i_0f_0}^{\text{eff}}(t)] \tag{17a}$$

or

$$\delta(t) = [2\Delta\omega_P(t) - S_{i_2g}^{\text{eff}}(t)] - [2\Delta\omega_S - S_{i_2f_2}^{\text{eff}}(t)]. \tag{17b}$$

For the case of population transfer to the final rovibrational level $v_f=2, J_f=2$ of the $X\,^1\Sigma_g^+$ state, we observe that the linear two-photon chirping curves slightly intersect the relative effective Stark shift curves during the rising of the pulses [Fig. 4(b)] and a little deviation of the chirp rate parameters (β_P, β_S) from the "global" value of 0.53 (or 0.529) occurs. Here, the optimal value of β_P, β_S is 0.521 for the maximum transfer of population to the final level $v_f=2, J_f=2$. The slight deviation from the global value of 0.53 (for a

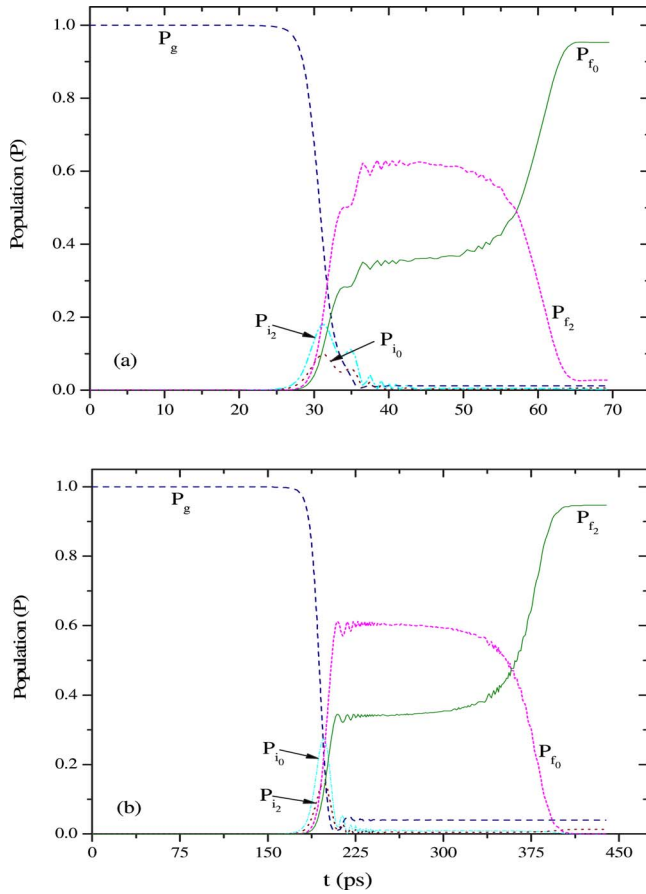FIG. 5. (Color online) Populations of the ground ($v_g = 0$, $J_g = 0$), resonant intermediate (v_i, J_i) and final (v_f, J_f) levels of Li$_2$ molecule as a function of time (t) with the optimal value of chirp rate parameters (β_P, β_S) for peak intensities $I_P^0 = 3.0 \times 10^{11}$ W/cm^2, $I_S^0 = 1.0 \times 10^{11}$ W/cm^2, and different pulse widths (τ_P, τ_S) of the pump and Stokes lasers. (a) $v_f = 1$, $J_f = 0$; $v_i = 1$, $J_i = 0$, $\tau_P = \tau_S = 35$ ps and $\beta_P = \beta_S = 0.53$. (b) $v_f = 1$, $J_f = 2$; $v_i = 1$, $J_i = 2$, $\tau_P = \tau_S = 220$ ps and $\beta_P = \beta_S = 0.529$.

three-level system [13]) may possibly occur due to the strong two-photon couplings $\widetilde{\Omega}_{i_0 i_2}$ and $\widetilde{\Omega}_{f_0 f_2}$ for the multilevel Li$_2$ system. Thus, in general, the strong two-photon couplings of the adjacent rotational levels cause a large change of the dressed energy values and consequently of the chirp rates necessary for optimal transfer. However, the optimal dimensionless chirp rate parameters (β_P, β_S) which determine the timing (T) of the resonance [$\delta(T) = 0$] remain almost the same, demonstrating the validity of the dynamical picture of the population transfer.

Figures 5 and 6 display the populations of the initial ground, resonant intermediate, and final levels as functions of time (t) for maximum population transfer at the end of the pulses to the final levels $v_f = 1$, $J_f = 0, 2$ and $v_f = 2$, $J_f = 0, 2$, respectively, with optimal values of the chirp rate parameters, pulse widths, and peak intensities. It is worth mentioning here that for maximum population transfer to the final levels $v_f = 1, 2$ with $J_f = 0$, we have made an initial ($t = 0$) two-photon resonance with the intermediate level $v_i = 1$ with $J_i = 0$ of the 2 $^1\Sigma_g^+$ state and have taken the chirp rates to be linearly proportional to the relative effective Stark shifts of
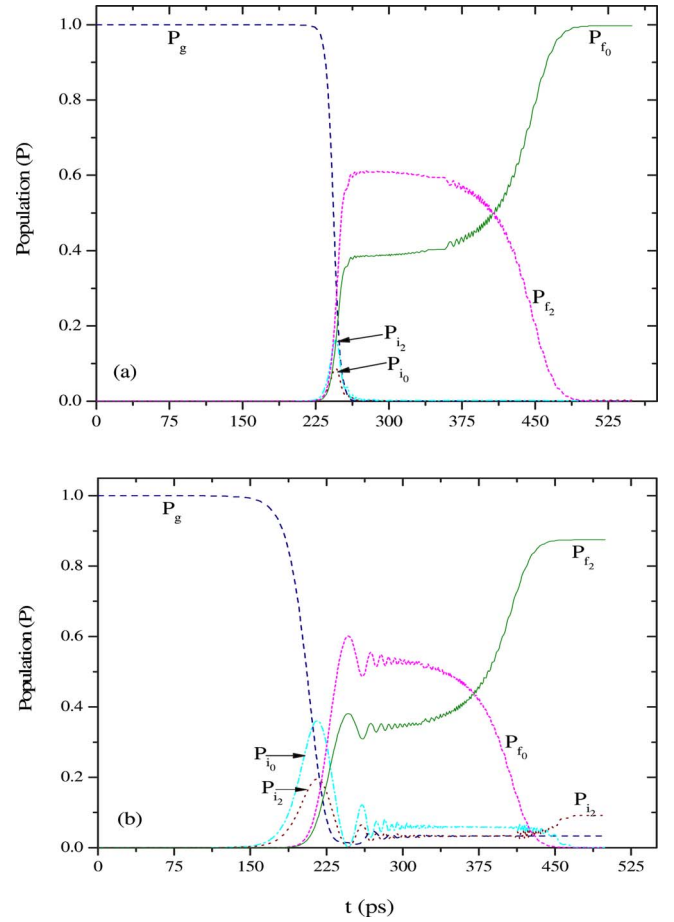
FIG. 6. (Color online) Same as Fig. 5 except for $I_P^0 = 1.0 \times 10^{11}$ W/cm^2, $I_S^0 = 1.5 \times 10^{10}$ W/cm^2 and (a) $v_f = 2$, $J_f = 0$; $v_i = 1$, $J_i = 0$, $\tau_P = \tau_S = 275$ ps and $\beta_P = \beta_S = 0.53$. (b) $v_f = 2$, $J_f = 2$; $v_i = 1$, $J_i = 2$, $\tau_P = \tau_S = 250$ ps and $\beta_P = \beta_S = 0.521$.

the corresponding levels at the peak intensities of the pulses. Hence, the two-photon chirpings, with optimal value of the chirp rate parameters (β_P, β_S), compensate the relative dynamic shifts at a time T (Figs. 3 and 4) during the rising of the pulses. This results in two-step [(2+2)-photon] Raman resonance, $\delta(T) = 0$, giving rise to maximum population inversion. For population transfer to the final levels $v_f = 1, 2$ with $J_f = 2$, we make two-photon resonance (at $t = 0$) with the intermediate resonant level $v_i = 1$ with $J_i = 2$ and the linear chirp rates are taken to be proportional to the relative effective Stark shifts of the corresponding levels at the peak intensities. Then, with optimal value of the chirp rate parameters and required pulse widths, we get maximum population transfer to the final target levels. We observe that when population transfer, at the end of the pulses, is maximum to the final levels $v_f = 1, 2$ with $J_f = 0$, an appreciable population also builds up in the final levels $v_f = 1, 2$ with $J_f = 2$ during the falling of the pulses and vice versa. However, at the termination of the pulses another reversal takes place and the population switches to the target rotational state level at the expense of the other allowed state level whose population becomes insignificant. This is certainly a simple consequence of the strong two-photon coupling between the rotational levels $J_f = 0$ and 2 of $v_f = 1, 2$. There is also some transient
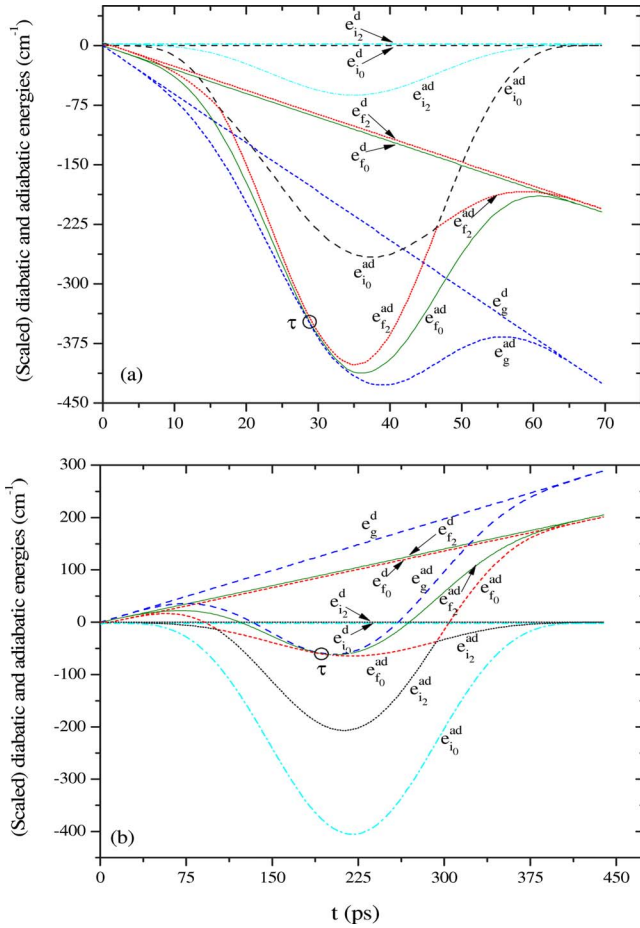
FIG. 7. (Color online) (Scaled) diabatic and adiabatic energy values of the ground ($v_g=0$, $J_g=0$), resonant intermediate (v_i, J_i), and final (v_f, J_f) levels of Li$_2$ molecule as a function of time (t) with the optimal value of chirp rate parameters (β_P, β_S) for peak intensities $I_P^0=3.0\times10^{11}$ W/cm^2, $I_S^0=1.0\times10^{11}$ W/cm^2, and different pulse widths (τ_P, τ_S) of the pump and Stokes lasers. (a) $v_f=1$, $J_f=0$; $v_i=1$, $J_i=0$, $\tau_P=\tau_S=35$ ps and $\beta_P=\beta_S=0.53$. (b) $v_f=1$, $J_f=2$; $v_i=1$, $J_i=2$, $\tau_P=\tau_S=220$ ps and $\beta_P=\beta_S=0.529$.

population transfer to the intermediate resonant rotational levels $J_i=0$ and 2 of $v_i=1$ near the peak of the pulses. The figures show that we can control the branching in population transfer to the final rotational levels $J_f=0$ (Q branch) and $J_f=2$ (S branch) of the fundamental ($v_f=1$) and first overtone ($v_f=2$) transitions by proper choice of laser parameters in the hyper-Raman process. In our numerical investigation, we have taken into account the dynamic Stark shifts (Table I) of the rotational levels ($J_g=0$, $J_i=0,2$, and $J_f=0,2$) of the model Li$_2$ molecular system (Fig. 1) and obtained maximum population inversion by choosing the optimal value of $\beta_P(\beta_S)$ (Table II). Thus, taking into consideration the full effect of molecular rotation including all the rotational coupling occurring through the radiation fields, it is possible to achieve efficient population transfer to a selective rovibrational level.

Figures 7 and 8 illustrate the (scaled) diabatic and adiabatic eigenenergies of the five relevant levels for the laser pulse widths and chirp rate parameters resulting in maximum population transfer to the final levels $v_f=1$ with $J_f=0,2$ and
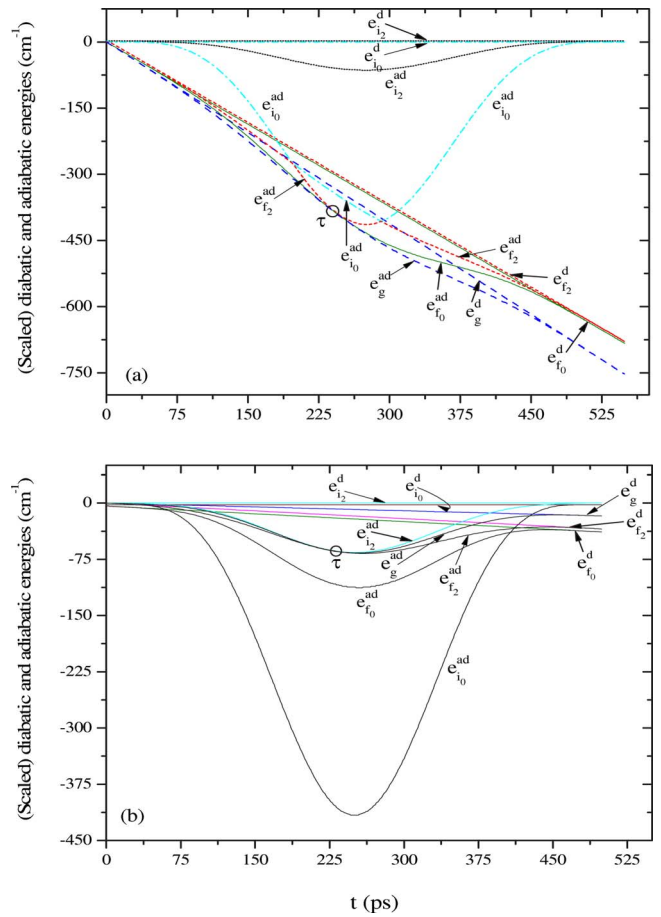
FIG. 8. (Color online) Same as Fig. 7 except for $I_P^0=1.0\times10^{11}$ W/cm^2, $I_S^0=1.5\times10^{10}$ W/cm^2 and (a) $v_f=2$, $J_f=0$; $v_i=1$, $J_i=0$, $\tau_P=\tau_S=275$ ps and $\beta_P=\beta_S=0.53$. (b) $v_f=2$, $J_f=2$; $v_i=1$, $J_i=2$, $\tau_P=\tau_S=250$ ps and $\beta_P=\beta_S=0.521$.

$v_f=2$ with $J_f=0,2$, respectively. When the adiabatic energies corresponding to the initial ground and the final rovibrational levels approach each other very closely (at the time τ), transfer of population from the initial to the final target levels begins due to nonadiabatic transition between the corresponding dressed (adiabatic) states. Thus, it is clear from the figures that due to simultaneous pulses and without any initial ($t=0$) detuning, the passage is not adiabatic and the population transfer takes place purely by a nonadiabatic passage through (nonadiabatic) transition between adiabatic states [13].

Figures 9 and 10 depict the populations of the relevant levels, at the end of the pulses, with dimensionless chirp rate parameter $\beta_P(\beta_S)$ for the final levels $v_f=1$ with $J_f=0,2$ and $v_f=2$ with $J_f=0,2$, respectively. It is seen that the final level population depends on $\beta_P(\beta_S)$ in an oscillatory manner approaching to 1 at a value of $\beta_P(\beta_S)$ equal or very close to the value of 0.53 which was obtained as the optimal value for maximum population transfer in a three-level molecular system [13]. We observe that the chirp rate parameter $\beta_P(\beta_S)$ controls and determines the population inversion from the ground to the final levels in a very sensitive way. Though the population transfer to the final rovibrational levels (Q and S branches) is very sensitive to the chirp rate, the population
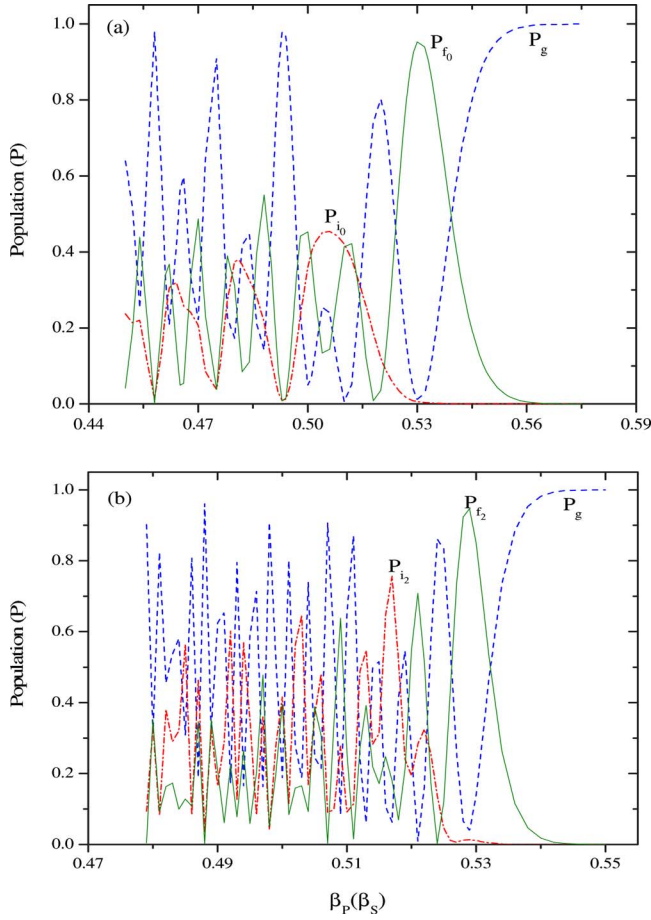
FIG. 9. (Color online) Populations of the ground ($v_g=0$, $J_g=0$), resonant intermediate (v_i,J_i) and final (v_f,J_f) levels of Li$_2$ molecule, at the end of the pulses, as a function of chirp rate parameter β_P (β_S) for peak intensities $I_P^0=3.0\times10^{11}$ W/cm^2, $I_S^0=1.0\times10^{11}$ W/cm^2 and different pulse widths (τ_P, τ_S) of the pump and Stokes lasers. (a) $v_f=1$, $J_f=0$; $v_i=1$, $J_i=0$, and $\tau_P=\tau_S=35$ ps. (b) $v_f=1$, $J_f=2$; $v_i=1$, $J_i=2$, and $\tau_P=\tau_S=220$ ps.

transfer (at the end of the pulses) is efficient for a small range of values close to the value 0.53 of the chirp rate parameter $\beta_P(\beta_S)$ (Figs. 9 and 10). We expect that the control of population transfer in Q and S branches would be experimentally feasible with the value of $\beta_P(\beta_S)$ near about 0.53 (Table II).

For the tailored pump laser wavelength (λ_P^0) of 992 nm, the rovibrational levels $v_r=1$, $J_r=1$ (3) of the excited electronic state 2 $^1\Sigma_u^+$ (with a double-well potential) [20] are almost in one-photon resonance with the rovibrational levels $v_i=1$, $J_i=0$ (2) of the resonant intermediate excited electronic state 2 $^1\Sigma_g^+$ (Fig. 1). But, due to the fact that the levels $v_r=1$, $J_r=1$ (3) lie in the outer well [20] of the potential of the 2 $^1\Sigma_u^+$ state, the transitions from the $v_i=1$, $J_i=0$ (2) to the $v_r=1$, $J_r=1$ (3) levels are highly non-Franck-Condon in nature (Table I). As a result, these transitions, though resonant, have no detrimental effect on the population transfer to the final target levels of our model Li$_2$ molecular system. It may be noted that since the dissipative term $\Gamma_{i_0}(\Gamma_{i_2})$ is much smaller than the two-photon Rabi frequencies or the Stark shifts (Table I) for the (peak) laser intensities considered, the
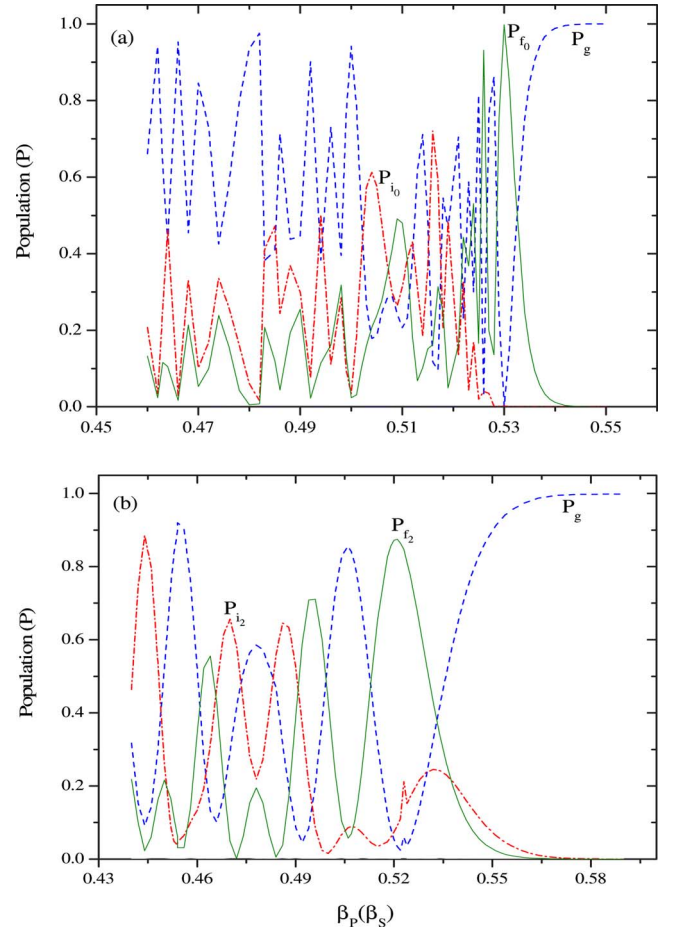

FIG. 10. (Color online) Same as Fig. 9 except for $I_P^0=1.0\times10^{11}$ W/cm^2, $I_S^0=1.5\times10^{10}$ W/cm^2 and (a) $v_f=2$, $J_f=0$; $v_i=1$, $J_i=0$, and $\tau_P=\tau_S=275$ ps. (b) $v_f=2$, $J_f=2$; $v_i=1$, $J_i=2$, and $\tau_P=\tau_S=250$ ps.

transfer remains the same in absence of the relaxation term and the chirp rate also does not change due to this dissipation.

We hope that with the advancement of current laser technology, experiments with chirped laser parameters similar to those used by us will be feasible. Existing Ti:sapphire laser would be suitable for the experiment.

V. CONCLUSION

We have investigated in detail the population transfer from the initial ground to higher rovibrational levels of a five-level Li$_2$ molecule by (2+2)-photon STIHRNAP process with linearly chirped pump and Stokes laser pulses. We have achieved almost complete population inversion to selective final target levels for different sets of laser parameters. The two-photon couplings between the closely spaced (rotational) levels of Li$_2$ have been considered to determine the required chirp rates for optimizing the population transfer. We have observed that the population inversion depends sensitively on the dimensionless chirp rate parameters. We have controlled the branching in population transfer to the final rotational levels $J_f=0$ (Q branch) and $J_f=2$ (S branch)

of the fundamental ($v_f=1$) and first overtone ($v_f=2$) transitions by properly choosing the laser parameters. We have endeavored to interpret the population transfer within the framework of the adiabatic energy eigenvalue picture and nonadiabatic passage between the adiabatic states. The present work is an application of a (2+2)-photon STIHR-NAP process to a model multilevel molecular system (Li_2) for selective and almost total population inversion from the initial ground to the final target rovibrational levels with chirped ir laser pulses.

[1] K. Bergmann, H. Theuer, and B. W. Shore, Rev. Mod. Phys. **70**, 1003 (1998); N. V. Vitanov, T. Halfmann, B. W. Shore, and K. Bergmann, Annu. Rev. Phys. Chem. **52**, 763 (2001), and references cited therein.

[2] Y. B. Band and P. S. Julienne, J. Chem. Phys. **94**, 5291 (1991); **95**, 5681 (1991); **97**, 9107 (1992); Y. B. Band, Phys. Rev. A **45**, 6643 (1992).

[3] N. V. Vitanov and S. Stenholm, Opt. Commun. **127**, 215 (1996); **135**, 394 (1997); Phys. Rev. A **55**, 648 (1997); **55**, 2982 (1997); **56**, 741 (1997); **56**, 1463 (1997).

[4] S. Ghosh, S. Sen, S. S. Bhattacharyya, and S. Saha, Phys. Rev. A **59**, 4475 (1999); Pramana, J. Phys. **54**, 827 (2000).

[5] L. P. Yatsenko, S. Guérin, T. Halfmann, K. Böhmer, B. W. Shore, and K. Bergmann, Phys. Rev. A **58**, 4683 (1998).

[6] S. Guérin, L. P. Yatsenko, T. Halfmann, B. W. Shore, and K. Bergmann, Phys. Rev. A **58**, 4691 (1998).

[7] K. Böhmer, T. Halfmann, L. P. Yatsenko, B. W. Shore, and K. Bergmann, Phys. Rev. A **64**, 023404 (2001).

[8] S. Chelkowski and G. N. Gibson, Phys. Rev. A **52**, R3417 (1995); S. Chelkowski and A. D. Bandrauk, J. Raman Spectrosc. **28**, 459 (1997).

[9] J. C. Davis and W. S. Waren, J. Chem. Phys. **110**, 4229 (1999), and references cited therein.

[10] S. Sen, S. Ghosh, S. S. Bhattacharyya, and S. Saha, J. Chem. Phys. **116**, 581 (2002).

[11] S. Thomas, S. Guérin, and H. R. Jauslin, Phys. Rev. A **71**, 013402 (2005).

[12] F. Légaré, S. Chelkowski, and A. D. Bandrauk, J. Raman Spectrosc. **31**, 15 (2000).

[13] C. Sarkar, R. Bhattacharya, S. S. Bhattacharyya, and S. Saha, J. Chem. Phys. **127**, 104304 (2007).

[14] A. A. Radzig and B. M. Smirnov, *Reference Data on Atoms, Molecules and Ions* (Spinger, New York, 1985), Vol. 31.

[15] S. Guérin, Phys. Rev. A **56**, 1458 (1997).

[16] C. Cohen-Tannoudji, B. Diu, and F. Laloë, *Quantum Mechanics* (Wiley, New York, 1977), Vol. 1, p. 407.

[17] P. Lambropoulos and X. Tang, in *Atoms in Intense Laser Fields*, edited by M. Gavrila (Academic, London, 1992).

[18] S. N. Dixit and P. Lambropoulos, Phys. Rev. A **27**, 861 (1983).

[19] S. Ghosh, S. Mitra, S. S. Bhattacharyya, and S. Saha, J. Phys. B **29**, 3109 (1996).

[20] I. Schmidt-Mink, W. Müller, and W. Meyer, Chem. Phys. **92**, 263 (1985).

[21] N. E. Greville, in *Mathematical Methods for Digital Computers*, edited by A. Ralston and H. S. Wilf (Wiley, New York, 1967), Vol. 2, p. 156.